Microbiota-driven vaccination in soft ticks: Implications for survival, fitness and reproductive capabilities in Ornithodoros moubata

Ana Laura Cano-Argüelles, Elianne Piloto-Sardiñas, Apolline Maitre, Lourdes Mateos-Hernández, Jennifer Maye, Alejandra Wu-Chuang, Lianet Abuin-Denis, Dasiel Obregón, Timothy Bamgbose, Ana Oleaga, et al.

Received: 7 March 2024 | Revised: 24 May 2024 | Accepted: 9 August 2024

DOI: 10.1111/mec.17506

ORIGINAL ARTICLE

MOLECULAR ECOLOGY WILEY

Microbiota-driven vaccination in soft ticks: Implications for survival, fitness and reproductive capabilities in *Ornithodoros moubata*

Ana Laura Cano-Argüelles[1] | Elianne Piloto-Sardiñas[2,3] | Apolline Maitre[3,4,5] | Lourdes Mateos-Hernández[3] | Jennifer Maye[6] | Alejandra Wu-Chuang[3] | Lianet Abuin-Denis[3,7] | Dasiel Obregón[8] | Timothy Bamgbose[9,10] | Ana Oleaga[1] | Alejandro Cabezas-Cruz[3] | Ricardo Pérez-Sánchez[1]

[1]Parasitology Laboratory, Institute of Natural Resources and Agrobiology (IRNASA, CSIC), Salamanca, Spain

[2]Direction of Animal Health, National Center for Animal and Plant Health, Carretera de Tapaste y Autopista Nacional, San José de las Lajas, Mayabeque, Cuba

[3]Laboratoire de Santé Animale, ANSES, INRAE, Ecole Nationale Vétérinaire d'Alfort, UMR BIPAR, Maisons-Alfort, France

[4]INRAE, UR 0045 Laboratoire de Recherches Sur Le Développement de L'Elevage (SELMET-LRDE), Corte, France

[5]EA 7310, Laboratoire de Virologie, Université de Corse, Corte, France

[6]SEPPIC Paris La Défense, La Garenne Colombes, France

[7]Animal Biotechnology Department, Center for Genetic Engineering and Biotechnology, Havana, Cuba

[8]School of Environmental Sciences, University of Guelph, Guelph, Ontario, Canada

[9]Microbiology Unit, Department of Biological Sciences, Kings University, Odeomu, Osun State, Nigeria

[10]National Agency for Food and Drug Control and Administration (NAFDAC), Isolo, Lagos State, Nigeria

Correspondence
Ricardo Pérez-Sánchez, Parasitology Laboratory, Institute of Natural Resources and Agrobiology (IRNASA, CSIC), Cordel de Merinas, 40-52, 37008 Salamanca, Spain.
Email: ricardo.perez@irnasa.csic.es

Alejandro Cabezas-Cruz, Laboratoire de Santé Animale, ANSES, INRAE, Ecole Nationale Vétérinaire d'Alfort, UMR BIPAR, Maisons-Alfort, F-94700, France.
Email: alejandro.cabezas@vet-alfort.fr

Funding information
Agence Nationale de la Recherche, Grant/Award Number: ANR-10-LABX-62-IBEID; European Regional Development Fund, Grant/Award Number: PID2022-136644OB-I00

Handling Editor: Sebastien Calvignac-Spencer

Abstract

The *Ornithodoros moubata* (Om) soft tick, a vector for diseases like tick-borne human relapsing fever and African swine fever, poses challenges to conventional control methods. With diminishing insecticide efficacy, harnessing the tick's microbiota through innovative approaches like microbiota-driven vaccination emerges as a promising strategy for sustainable and targeted disease control. This study investigated the intricate relationship between *Pseudomonas*, a keystone taxon in the Om microbiome, and its impact on tick fitness, microbiome structure and network dynamics. Utilizing in silico analyses and empirical vaccination experiments, the role of *Pseudomonas* within microbial networks in the tick midguts (MG) and salivary glands (SG) of Om was studied. Additionally, the consequences of anti-microbiota vaccines targeting *Pseudomonas* and *Lactobacillus* on tick fitness, microbiome diversity and community assembly were explored. The result of the study shows that in Om, *Pseudomonas* plays a central role in microbial networks, influencing keystone species despite being categorized as peripheral (interacting with 47 different taxa, 13 of which are keystone

Ana Laura Cano-Argüelles and Elianne Piloto-Sardiñas equal contribution.

species). Anti-microbiota vaccination targeting *Pseudomonas* and *Lactobacillus* yields distinct effects on tick fitness, with *Pseudomonas* vaccination significantly impacting female tick survival, while *Lactobacillus* significantly reduced oviposition and fertility. Microbiome changes post-vaccination reveal diversity alterations, emphasizing the impact of vaccine choice. Community assembly dynamics and network robustness analyses highlight *Pseudomonas*' pivotal role, in influencing topological features and network resilience. The findings of the study provide comprehensive insights into the intricate dynamics of Om microbial networks and the potential of targeted microbiota-driven vaccines for tick control.

KEYWORDS
anti-microbiota vaccine, community assembly, *Ornithodoros moubata*, tick microbiome

1 | INTRODUCTION

The African hut tampan, *Ornithodoros moubata* (Om), poses a significant public health threat across sub-Saharan Africa. This soft tick acts as a vector for several debilitating diseases, including tick-borne human relapsing fever (TBRF) caused by the spirochete *Borrelia duttoni* and African Swine Fever (ASF) (Cutler et al., 2009). The parasitic arthropod's ability to thrive in diverse environments raises a significant challenge to conventional control strategies. Traditional control methods often rely on insecticides, but their effectiveness is waning due to resistance development and environmental concerns. Their presence may affect the eradication of TBRF and ASF from endemic areas (Diaz-Martin et al., 2015). In recent years, the intricate interplay between microbial communities and their host organisms has become a focal point of scientific inquiry, unlocking new avenues for innovative approaches to disease control (Qi et al., 2024; Zheng et al., 2020).

One promising strategy lies in harnessing the power of the Om's own microbiota—the diverse community of microorganisms residing within its gut. Recent research suggests that manipulating these microbial communities can have profound effects on the tick's fitness and ability to transmit diseases (Mateos-Hernández et al., 2021; Wu-Chuang et al., 2023). This approach, known as microbiota-driven vaccination, holds immense potential for developing sustainable and targeted interventions against ticks (Maitre et al., 2022). In the dynamic world of tick microbiomes, certain key microorganisms, known as keystone taxa, play a pivotal role in shaping the diversity, composition and assembly of the microbial community (Mateos-Hernández et al., 2021; Wu-Chuang et al., 2021, 2022). Unlike traditional microbiome alteration strategies, immunization of hosts with keystone taxa from the tick's microbiota offers a targeted way to modify the microbial community (Mateos-Hernández et al., 2021), reduce tick fitness (Mateos-Hernández et al., 2020) and reduce vector competence (Maitre et al., 2022).

This influence is distinct from other microbiome perturbation strategies, such as paratransgenesis (Pavanelo et al., 2023). Selecting a keystone taxon for the development of anti-microbiota vaccine involves several key steps: pinpointing bacterial nodes with significant connections in microbial co-occurrence networks, finding bacteria that are widespread among tick microbiomes, and identifying those with high abundance (Mateos-Hernández et al., 2020; Wu-Chuang et al., 2022). The efficacy of focusing on tick microbiome, particularly keystone taxa and other relevant nodes, through host antibodies (Maitre et al., 2022), has been tested in silico, showing that targeting these central nodes weakens the microbial network (Maitre et al., 2023).

Furthermore, studies involving animal models have confirmed that targeting a keystone taxon reduces the alpha-diversity within the tick microbiome and affects its community assembly (Mateos-Hernández et al., 2021; Wu-Chuang et al., 2023). Empirical evidence shows that hard ticks feeding on hosts immunized with microbiota-driven vaccines experienced changes in the microbiome, leading to lower level of the pathogen *Borrelia afzelii* in *Ixodes ricinus* tick (Wu-Chuang et al., 2023). Similar outcomes were observed in mosquitoes, where the presence and abundance of *Plasmodium relictum* were reduced in the midguts of *Culex quinquefasciatus* mosquitoes that fed on microbiota-immunized canaries (Aželytė et al., 2022). These findings in hard ticks and mosquitoes hint at the wider applicability of microbiota-driven vaccines against other blood-feeding parasites, including its potential in soft ticks.

Analyses of the microbiomes in the midgut (MG) and salivary glands (SG) of Om and *Ornithodoros erraticus* (Oe) from a tick colony revealed distinct microbial communities specific to species and tissues (Piloto-Sardiñas et al., 2023). Despite significant differences in microbial community diversity and stability between Om tissues (MG-SG), the discovery of shared keystone taxa and consistent patterns across tissues points to potential microbiota-driven vaccine candidates capable of altering tick physiology and pathogen colonization (Piloto-Sardiñas et al., 2023).

This study seeks to explore the hypothesis that altering keystone taxa trough microbiota-driven vaccination can influence both the fitness and microbial community of Om. To achieve this, an in-depth analysis of how a previously identified keystone taxon, found in the midgut and salivary glands of Om (MG-SG) (Piloto-Sardiñas

et al., 2023) assembles within the tick was performed. Afterwards, the microbiome was assessed following both theoretical (in silico) and real-world (in vivo) manipulations to determine its suitability as a candidate for a microbiota-driven vaccine. The findings suggest that vaccines targeting the microbiome offer a promising strategy for creating new vaccines aimed to control soft tick populations and the diseases they transmit.

2 | MATERIALS AND METHODS

2.1 | Selection of target taxon for anti-microbiota vaccine development

A previous study showed that the diversity, composition, abundance and assembly of microbial communities associated with *O. moubata* (Om) are tissue-specific, suggesting different interaction patterns in OmMG and OmSG (Piloto-Sardiñas et al., 2023). During this study, keystone microbial taxa were identified, highlighting *Pseudomonas* as a common keystone taxon present in both tissues (Piloto-Sardiñas et al., 2023). The positioning of *Pseudomonas* as a common keystone taxon in both tissues suggested an important role of the microorganism within the community since in theory the taxon faced different conditions and was still capable of carrying out an effective colonization process. The prominence of *Pseudomonas* within these microbiomes suggested it plays a significant role in community assembly, vector fitness and/or pathogen colonization.

These factors make *Pseudomonas* a prime target for developing an anti-microbiota vaccine. To explore the hypothesis that targeting *Pseudomonas* would influence the microbial community structure and affect tick health, in silico analyses based on data from a previous study (Bioproject PRJNA931807) (Piloto-Sardiñas et al., 2023) were initially performed, aiming to have a better understanding of *Pseudomonas*' impact on the Om microbial community.

Following this, the focus of the vaccine development was on *Pseudomonas*, while *Lactobacillus* was abundant within the community but did not meet the criteria to be considered a keystone taxon. The microorganism was selected as a point of comparison, control and to analyse in vivo the consequences for the community of manipulating an abundant but non-keystone taxon. The effects of immunizing rabbits with either the *Pseudomonas* or *Lactobacillus* vaccine on tick fitness and the microbial communities within ticks that fed on these rabbits were assessed (Figure 1). An overview of the study is displayed in Figure 1.

2.2 | *Pseudomonas* connectivity in OmMG and OmSG networks

To investigate how *Pseudomonas* taxon integrates into the microbial community of Om, specifically within the MG and SG, both their positive and negative interactions with other bacteria in the microbiome were examined. Sub-networks from larger global co-occurrence networks (Piloto-Sardiñas et al., 2023) were generated to visualize these interactions (Piloto-Sardiñas et al., 2023). The analysis was carried out in Gephi v0.10 (Bastian et al., 2009), with the connections between microbes quantified using Sparse Correlations for Compositional (SparCC) (SparCC >0.75 or <−0.75) (Friedman & Alm, 2012) in R v.4.3.1 (R Core Team, 2023), using RStudio (RStudio Team, 2020) (File S1).

2.3 | Centrality measures in networks of OmMG and OmSG microbiome

To understand the structure of the microbiome networks within OmMG and OmSG, the analysis was focused on the distribution of centrality measures across different taxa, including *Pseudomonas* and others within these networks. This analysis was conducted to assess the roles that various taxa play within the network, using measures of within-module (Zi) and among-module (Pi) connectivity (Guimerà & Nunes Amaral, 2005). These measures help categorize the taxa into four distinct roles based on their connectivity:

- Peripheral taxa: Taxa that have limited connections within their own module and minimal interactions with other modules, characterized by Zi ≤2.5 and Pi ≤0.62.
- Connectors: Taxa that primarily link different modules together, identified by Zi ≤2.5 but with a higher Pi >0.62, indicating their role in connecting disparate parts of the network.
- Module hubs: Highly connected taxa within their own module but not significantly connected to other modules, marked by Zi >2.5 and Pi ≤0.62.
- Network hubs: Taxa that serve as central connectors both within their own module and across the entire network, with high connectivity indicated by Zi >2.5 and Pi >0.62.

The thresholds of 2.5 and 0.62 are standard values defined by Guimerà and Nunes Amaral (2005). For each taxon within the network, Zi and Pi values were calculated considering only positive interactions. The calculations were performed using the 'code-zi-pi-plot' package (Cao et al., 2018; Guo et al., 2022) in R v.4.3.1 (R Core Team, 2023), using RStudio (RStudio Team, 2020) (File S2). The resulting network structures and the positions of taxa within them were then visualized using GraphPad Prism version 8.0.1 (GraphPad Software, San Diego, CA, USA). This approach allows to identify key players in the microbial community of Om and understand how they interact within and across different modules of the network.

2.4 | Module composition in OmMG and OmSG

The analysis of the module composition was performed both in the presence of *Pseudomonas* and after its removal to assess its impact. The equivalence of modules within the Om (MG-SG) networks was maintained consistent, resulting in the identification of two main

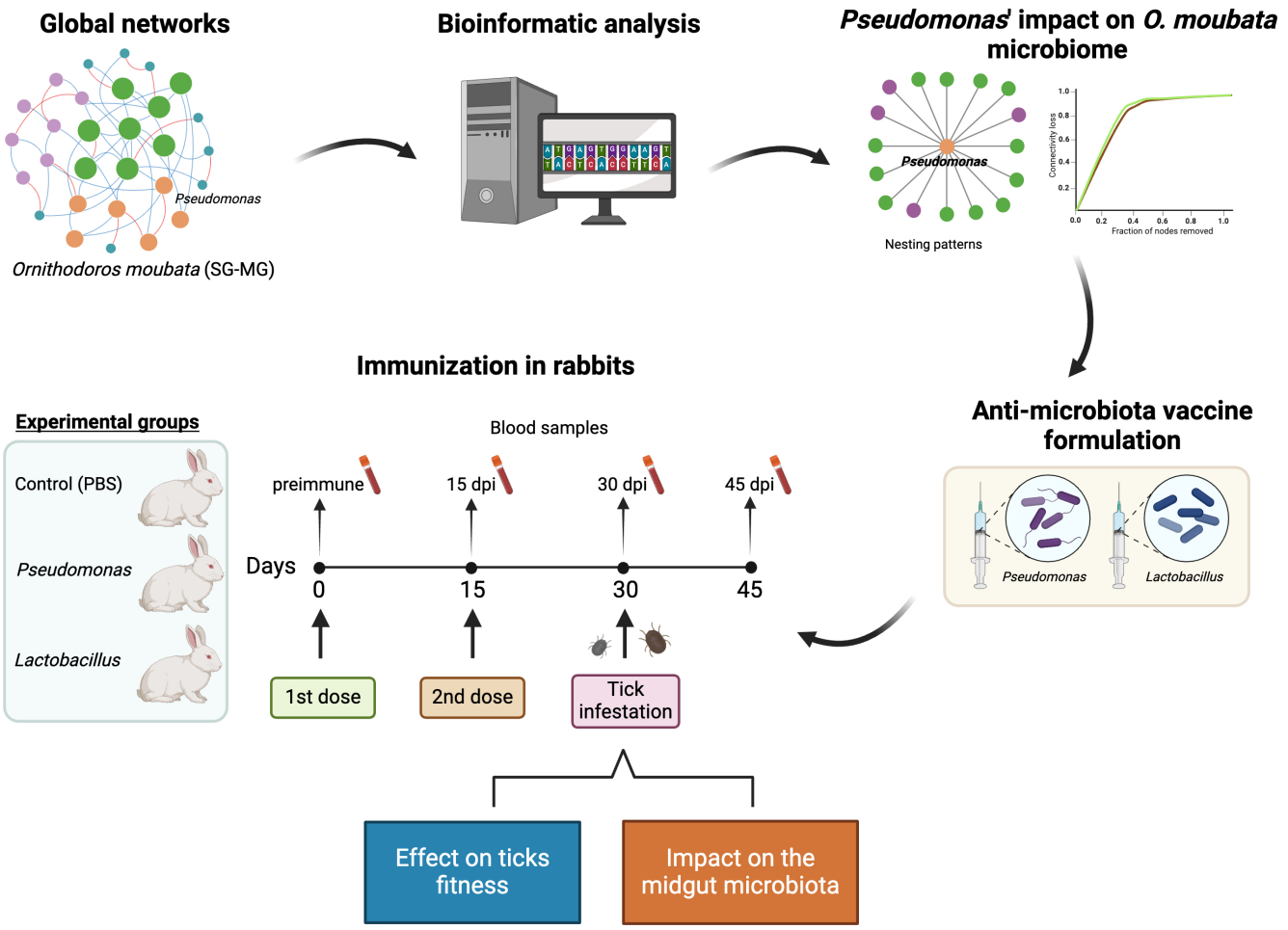

FIGURE 1 Experimental design for testing of anti-microbiota vaccines. Three groups of rabbits were given two doses (days 0 and 15) of live bacteria vaccine containing *Pseudomonas* (1×10^6 colony-forming units (CFU)) or *Lactobacillus* (1×10^6 CFU) or with a mock vaccine (PBS). At day 30, 45 female and 40 male adult *Ornithodoros moubata* ticks were allowed to feed on each rabbit for a 1-h period. Blood was collected at different point times as shown, and engorged ticks were used for vaccine efficacy and microbiome analysis.

modules: M1, which included *Pseudomonas*, and M2, characterized by greater taxonomic diversity and a higher modularity value. To better understand the influence of *Pseudomonas* on the network's assembly and module composition, sub-networks in presence (wP) and after taxon's removal (woP) were constructed. The relationships and distinctions between the modules were visually represented through Venn diagrams, utilizing the online tool available at http://bioinformatics.psb.ugent.be/webtools/Venn/. To represent microbial taxa shared between the wP and woP sub-networks, core association networks (CANs) were created, using a software toolbox, anuran (a toolbox with null models for identification of nonrandom patterns in association networks) (Röttjers et al., 2021), and this version was tested in Python 3.6.

2.5 | Robustness analysis using nodes removal and addition

The resilience of the network to disruptions through both the removal and addition of nodes, specifically focusing on changes within the OmMG and OmSG networks before and after the in silico removal of *Pseudomonas* was studied. To evaluate the network's robustness to node removal, the Network Strengths and Weaknesses Analysis (NetSwan) package (Lhomme, 2015) was utilized in R v.4.3.1 (R Core Team, 2023), using RStudio (RStudio Team, 2020; File S3). This involved calculating the fraction of nodes that needed to be removed to cause a connectivity loss of 80%, following both directed (e.g. based on betweenness, cascading effects and degree centrality) and random removal strategies.

To examine how the network responded to the addition of nodes, the Network Analysis and Visualization package was employed (Freitas et al., 2021) in R v.4.3.1 (R Core Team, 2023), using RStudio (RStudio Team, 2020; File S4). Network connectivity was quantified using two metrics: the degree metric of the largest connected component (LCC) and the average path length (APL), the nodes were incrementally added in sections ranging from 50 to 500. To analyse the significance of differences in LCC and APL before and after node addition, a Wilcoxon signed-rank test was conducted. The resulting *p*-values were then adjusted using the Benjamini–Hochberg procedure to minimize the false discovery rate. Bootstrapping techniques

were also implemented to generate confidence intervals for these metrics. Significance level was set at $p < .05$ to determine statistical relevance.

2.6 | Experimental evaluation of anti-microbiota vaccines on *O. moubata*

To empirically assess the impact of altering microbial taxa through vaccination, experiments focusing on tick fitness and midgut microbial community structure of OmMG were conducted. The experiments were carried out using ticks fed on rabbits that had been immunized with either a vaccine targeting *Pseudomonas*, a key microbial player identified as a prime candidate for anti-microbiota vaccine development, or *Lactobacillus*, which was chosen as a control due to its minor role in the Om microbiome. This approach allowed direct investigation of the effects of immunization against these specific microbes on the tick's fitness and its microbial community structure.

For bacteria immunization, *Pseudomonas aeruginosa* (ATCC 27853) was selected considering that it is a reference bacterial strain used in antibiotic susceptibility testing and quality control, while *Lactobacillus casei* was selected because despite being a species of probiotic bacteria, it is characterized by generating innate and adaptive immune responses in the host.

2.6.1 | Bacterial growth

The bacterial strains *Pseudomonas aeruginosa* (ATCC 27853) and *Lactobacillus casei* (Acedo-Felix & Gaspar Perez-Martınez, 2003) were grown in 50 mL of Luria Broth (Sigma-Aldrich, St. Louis, MO, USA) at 37°C until they reached an optical density (OD 600) of 1. The cultures were then washed twice with phosphate-buffered saline (PBS) (Sigma-Aldrich). Following this, the bacteria were centrifuged at 1000×*g* for 5 min, resuspended in PBS, and thoroughly mixed using a glass homogenizer with 20 strokes to ensure a uniform suspension. All steps in the preparation of the bacteria were carried out under sterile conditions to prevent contamination.

2.6.2 | Live bacteria immunization in rabbits

To create the live bacteria vaccine, 1×10^6 colony-forming units (CFU) of either *Pseudomonas aeruginosa* (ATCC 27853) or *Lactobacillus casei* (Acedo-Felix & Gaspar Perez-Martınez, 2003) were blended with a water-in-oil emulsion enriched with 70% Montanide™ ISA 71 VG adjuvant (Seppic, Paris, France). Subsequently, 500 µL of each of these formulations was subcutaneously administered to a group of three New Zealand white rabbits per candidate. A vaccine booster was administered 15 days following the initial dose. As part of the control group, an additional three rabbits received a treatment comprising PBS and adjuvant.

Blood samples were systematically collected from all experimental animals at distinct time intervals: pre-immune (before the first vaccine dose), at 15 days post-immunization (dpi) with the first dose, 30 dpi (15 days after the second dose and prior to tick infestation) and 45 dpi (30 days after the second dose and 15 days following the tick challenge). These collected samples were left 2 h incubating at room temperature to facilitate clotting, after which sera were extracted and stored at −20°C.

New Zealand White rabbits were purchased to a commercial supplier: Granja San Bernardo (Tulebras, Navarra (Spain), www.granjasanbernardo.com). All rabbits were 7 weeks old females, around 1.5 kg at the beginning of the experiment, reared by the Minimal Disease Level system, which guarantees Specific Pathogen-Free animals.

2.7 | Humoral response analysis

2.7.1 | Bacterial total protein extraction

To extract total proteins from *Pseudomonas* and *Lactobacillus* bacterial cells, a series of steps were carried out for optimal results. Initially, the bacterial cells underwent a thorough double wash in PBS. Subsequently, these cells were subjected to centrifugation at 1000×*g* for 5 min at 4°C. Following this, the resulting pellet of cells was carefully resuspended in a lysis buffer composed of 1% Triton-PBS (Sigma-Aldrich). For effective disruption of cellular material, mechanical homogenization was carried out using a sterile 26G needle.

The resulting homogenate was subjected to another round of centrifugation at 300×*g* for 5 min at 4°C, yielding a supernatant that was meticulously collected for subsequent analysis. To determine the protein concentration in this supernatant, the Bradford Protein Assay (Thermo Scientific, San Jose, CA, USA) was employed, utilizing bovine serum albumin as the reference standard.

2.7.2 | Enzyme-linked immunosorbent assay (ELISA)

Prior to tick infestation, the antibody titres of immune sera against bacterial total proteins from *Pseudomonas* and *Lactobacillus* was assessed using a serial dilution ELISA, following established protocols (Carnero-Morán et al., 2023; García-Varas et al., 2010). ELISA plates were coated with 50 ng of bacterial proteins per well, diluted in 100 µL of 0.05 M carbonate/bicarbonate buffer (pH 9.6). Serum dilutions in TPBS buffer (phosphate-buffered saline supplemented with 0.05% Tween 20) were prepared using a twofold dilution method, ranging from 1/50 to 1/6400. Additionally, anti-rabbit IgG-peroxidase (Sigma-Aldrich) was used at a dilution factor of 1/10,000. All incubation steps were performed at 37°C. Orthophenylenediamine was employed as the chromogenic substrate for peroxidase, and the reaction was stopped by adding 50 µL of 3 N sulphuric acid. Sample OD was measured at a wavelength of 492 nm. The serum titre was determined as the highest dilution

at which the reactivity exceeded twice the dilution of the corresponding pre-immune serum.

Afterwards, to assess the reactive antibody levels to bacterial proteins at each time point of the experiment, we used the same ELISA protocol. In this case, the sera from both vaccinated rabbits and the control group were diluted at a ratio of 1/100 in PBS. The rest of protocol was executed as described above.

2.8 | Tick infestation with *O. moubata*

The tick specimens utilized in this study were from a laboratory colony maintained at the Institute of Natural Resources and Agrobiology of Salamanca (IRNASA-CSIC, Salamanca, Spain). These ticks were initially provided by the Institute for Animal Health (Pirbright, Surrey, UK) and originally sourced from Malawi. The tick colonies were regularly fed on New Zealand white rabbits and were carefully controlled under specific conditions, which included maintaining a constant temperature of 28°C, a relative humidity level of 85% and adhering to a 12-h light–dark cycle.

Fifteen days following the final administration of the antigen dose (30 dpi), nine uniform groups (one for each rabbit) were organized, each consisting of 45 newly moulted female and 40 male adult Om ticks. These ticks were individually weighed and subsequently allowed to feed on rabbits for a period of 1 h. During this time frame, most ticks successfully completed their feeding, and any tick that remained attached to the host animal was promptly removed. Fed ticks were kept under controlled conditions: 28°C temperature and 85% humidity.

The ticks were divided into two distinct groups 48 h after feeding. The first group consisted of nine batches, with each one comprising 15 females and 30 males per rabbit. These specimens were weighed and checked for survival after feeding. Subsequently, each female tick was paired with two male ticks to facilitate mating and reproduction under controlled conditions. The second group, comprising 60 randomly selected females from each vaccination group, had their midguts carefully extracted in a cold (4°C) PBS solution and were then stored at −20°C for subsequent analysis. Before this procedure, the ticks underwent a series of meticulous washes using various solutions, including tap water, 3% hydrogen peroxide, two rinses in distilled water, 70% ethanol, and an additional two rinses in distilled water. All procedures were executed using sterile materials to prevent any potential contamination of the samples.

2.9 | Vaccine efficacy calculation

To assess the impact of the vaccine on these tick specimens, several parameters were evaluated, including survival (the percentage of ticks alive after feeding), ingested blood volume (determined by measuring the weight difference before and 48 h after feeding), female oviposition (the count of eggs laid per female) and fertility (the count of newly hatched nymphs-1 per female). The results for these parameters were presented as the mean ± standard deviation per group. Vaccine efficacy (E) for each antigen was calculated using the following formula: $E = 100 \times [1 - (S \times F)]$, where '$S$' and '$F$' represent reductions in the survival and fertility of female ticks.

2.10 | Statistical analysis

Comparative analysis of antibody levels was conducted through the following statistical methods. For the comparison between control and immunized rabbits, a two-way ANOVA was utilized. This was followed by pairwise comparisons, achieved using the Bonferroni test. These analyses were performed using GraphPad Prism 10 software (GraphPad Software, Boston, MA, USA). To assess the vaccine's impact on ticks that had fed on vaccinated rabbits, a one-way ANOVA was employed. Post hoc analysis was carried out using Dunnett's T-test. Significance was set at $p < .05$. These statistical analyses were conducted using SPSS version 29 software (IBM, Armonk, USA).

2.11 | Tick genomic DNA extraction

To extract genomic DNA, the NucleoSpin® Tissue Kit (Macherey-Nagel, Germany) as per the manufacturer's guidelines was used. Specifically, 10 pools per vaccination group were processed, each comprising six individual midguts from fed female Om ticks.

The procedure involved resuspending all samples in T1 buffer and Proteinase K, followed by mechanical homogenization using a T 25 digital ULTRA-TURRAX® (IKA, Germany). Subsequently, these samples were incubated overnight at 56°C.

The quality and concentration of DNA was determined using the NanoDrop 2000c (Thermo Scientific, USA) and agarose gel electrophoresis. As a control for the DNA extraction process, five PBS samples were also processed, following the same conditions and steps as the midgut samples.

2.12 | 16S rRNA amplicon sequencing and sequence processing

The library preparation and sequencing of the bacterial 16S rRNA gene were carried out at Novogene Bioinformatics Technology Co. in London, UK. For library preparation, up to 200 ng of DNA was utilized with a concentration exceeding 20 ng/μL. Libraries were constructed using the NEBNext® Ultra™ II DNA Library Prep Kit from New England Biolabs, located in Ipswich, MA, USA. Sequencing was conducted on a single lane of the Illumina MiSeq system, generating 251-base paired-end reads targeting the variable region V4 of the 16S rRNA gene. This was achieved by utilizing barcoded universal primers (515F/806R). The raw 16S rRNA sequences obtained from OmMG have been deposited in the SRA repository under the

Bioproject accession no. PRJNA1035006. Additionally, DNA amplification was performed on the extraction controls, following the same conditions as the other samples.

Subsequently, the raw sequences underwent demultiplexing to create FASTQ files. These files were then subjected to denoising, quality trimming, and merging processes using DADA2 (Callahan et al., 2016), a tool implemented within the QIIME 2 pipeline (version 2021.4; Bolyen et al., 2019). To mitigate the impact of potential contaminants originating from tissue processing and DNA extraction, the Decontam R package (Davis et al., 2018) was employed, utilizing a prevalence-based method with a threshold set at 0.5.

Amplicon sequence variants (ASVs) were aligned using the q2-alignment tool of MAFFT (Katoh & Standley, 2013), and a phylogenetic tree was constructed using the q2-phylogeny tool of FastTree 2 (Price et al., 2010). Taxonomic classifications were assigned to the ASVs using a classify-sklearn naïve Bayes taxonomic classifier, which was built upon the SILVA database (release 138; Quast et al., 2012) and the 515F/806R primer set. The resulting taxonomic data table was aggregated at the genus level and used for the assessment of bacterial diversity and network analysis.

2.13 | Bacterial taxonomic diversity, composition and differential relative abundance

Microbial comparisons in the OmMG microbiome were made between the groups vaccinated with *Pseudomonas* (OmMG-P) and *Lactobacillus* (OmMG-L) and the control (OmMG-C) group. Various alpha and beta diversity metrics were used for analysis, employing the q2-diversity plugin in QIIME 2 (Bolyen et al., 2019). Alpha diversity metrics, which assess within-group diversity, were determined using the observed features (DeSantis et al., 2006) and Faith's phylogenetic diversity index (Faith, 1992) to measure richness. Evenness was assessed using Pielou's evenness index (Pielou, 1966). Differences in alpha-diversity metrics between groups were assessed with the Kruskal–Wallis test ($p < .05$) within QIIME 2 (Bolyen et al., 2019).

For beta diversity, which evaluates between-group diversity, we employed the Bray Curtis dissimilarity index (Bray & Curtis, 1957) and performed a PERMANOVA test ($p < .05$) in QIIME 2. Beta dispersion was calculated using the betadisper function and the Vegan script implemented in RStudio (Oksanen et al., 2021; RStudio Team, 2020) with an ANOVA test ($p < .05$) for statistical analysis (File S5). Cluster analysis was conducted using the Jaccard coefficient of similarity within Vegan (Oksanen et al., 2021) implemented in RStudio (RStudio Team, 2020; File S6). Unique and shared taxa among the three conditions were visualized using Venn diagrams created with an online tool (http://bioinformatics.psb.ugent.be/webtools/Venn/).

To assess differences in taxa relative abundance among the three conditions, a Kruskal-Wallis test ($p < .05$) was used and implemented it using the ANOVA-Like Differential Expression (ALDEx2) package (Fernandes et al., 2013) on RStudio (RStudio Team, 2020; File S7). Only taxa with significant differences ($p < .05$) were selected for representation of the differential taxa relative abundance. Relative abundance values were transformed using the centred log ratio (clr) transformation. The identified differentially abundant taxa were used to generate a heatmap using the 'Heatplus' package in RStudio (RStudio Team, 2020; File S8).

2.14 | Co-occurrence networks analysis

Co-occurrence networks for each group were created by utilizing taxonomic information at the genus level. To compute the correlation matrices, the SparCC method (Friedman & Alm, 2012) implemented in RStudio (RStudio Team, 2020) was employed. The visualization of bacterial networks and the calculation of various topological parameters, such as the number of nodes and edges, weighted degree, network diameter, modularity, and clustering coefficient, were conducted using Gephi v.0.10.1 (Bastian et al., 2009). In these networks, each node represented a taxon, and edges indicated either positive correlations (SparCC >0.50) or negative correlations (SparCC <0.50) between the nodes.

The colours of nodes are assigned by the modularity class metric values, and the node size is proportional to the eigenvector centrality of each taxon. The colours in the edges represent strong positive (blue) or negative (red) correlations. The unique and shared nodes between groups were represented with Venn diagrams (http://bioinformatics.psb.ugent.be/webtools/Venn/).

2.15 | Comparative bacterial networks

The network comparisons were conducted using the Network Construction and Comparison for Microbiome Data (NetCoMi) R package (Peschel et al., 2021) in R v.4.3.1 (R Core Team, 2023), using RStudio (RStudio Team, 2020; File S9). To measure the dissimilarities between nodes in the vaccinated groups' networks and those in the control group, we calculated Jaccard indices for various centrality measures, such as degree, betweenness centrality, closeness centrality, eigenvector centrality and hub taxa. 'Most central nodes' refer to those with centrality values exceeding the 75th percentile of the empirical values.

The Jaccard index ranges from 0 (completely dissimilar sets) to 1 (identical sets). The probabilities were also computed, represented as $P(J \leq j)$ and $P(J \geq j)$, which indicate the likelihood of obtaining a Jaccard index 'j' or less and 'j' or greater, respectively, for the given total number of taxa in both sets, compared to random calculations. Furthermore, the Adjusted Rand Index (ARI) was calculated, which varies from −1 to 1. A positive ARI value suggests greater similarity of clustering, while a negative value implies less similarity than expected. All analyses were performed in RStudio (RStudio Team, 2020).

Additionally, in Gephi v0.10 (Bastian et al., 2009), sub-networks were constructed to highlight the local connectivity of *Pseudomonas*

and *Lactobacillus* within the global networks of the vaccinated (OmMG-P and OmMG-L) and control (OmMG-C) groups.

2.16 | Network tolerance to node removal and addition

A comprehensive analysis of tolerance to node removal and addition was conducted between OmMG-P, OmMG-L and OmMG-C networks. The network's robustness to node removal was evaluated after directed (betweenness, cascading and degree) and random attacks using the NetSwan package (Lhomme, 2015), implemented in RStudio (RStudio Team, 2020). Furthermore, the robustness of microbial coexistence networks to the addition of nodes was explored using Network Analysis and Visualization package (Freitas et al., 2021), the nodes were added gradually in sections ranging from 5 to 100. Both analyses were carried out following the procedures described in the Section 2.5.

3 | RESULTS

3.1 | Nesting patterns of *Pseudomonas* in *O. moubata* microbiome

To explore the hypothesis that targeting *Pseudomonas*, a keystone taxon in the Om microbiome (Piloto-Sardiñas et al., 2023), would influence the microbial community structure, *in-silico* analyses were initially performed based on data from a previous study on Om microbiome (Piloto-Sardiñas et al., 2023; Figure 1). The primary focus was on understanding how *Pseudomonas* interacts with other microbes within the MG and SG of Om.

The findings from the study underscored the significance of *Pseudomonas* within these microbial networks. Specifically, in the MG, *Pseudomonas* was found to interact with 47 different taxa (Figure 2a), 14 of which were keystone (Table S1). In the SG, it connected with 17 taxa (Figure 2b), with five keystones (Table S1). Additionally, when examining the distribution of connections (Zi and Pi connectivity), a similar pattern in both MG (Figure 2c) and SG (Figure 2d) was observed: most microbes, *Pseudomonas* included, were categorized as peripheral, indicating that they did not serve as central hubs within their respective networks.

To further understand *Pseudomonas*'s role, the effects of its removal from sub-networks formed by modules M1 (the module where *Pseudomonas* was located) and M2 (the module with the highest modularity in the global network) were examined. The OmMG sub-network with *Pseudomonas* (wP, Figure 2e) had topological changes, compared to that of the sub-network without *Pseudomonas* (woP, Figure 2f; Table S2). This distinction was further evident in the composition of modules (M1–M2) as each module displayed unique nodes in the presence or absence of *Pseudomonas* (Figure 2g; Table S3). Shared nodes between the two networks (OmMG-wP and OmMG-woP) that maintained the nature of their connectivity were represented by a CAN (Figure 2h). A similar trend was observed in OmSG, where topological changes were evident in OmSG-wP (Figure 2i) and OmSG-woP (Figure 2j; Table S2), alongside variations in module composition (Figure 2k; Table S3). The connectivity maintained between the nodes shared by both networks was represented in a CAN (Figure 2l).

Despite the removal of *Pseudomonas*, the networks remained robust, showing little change in their ability to withstand connectivity loss after both random (Figure S1A,B) and directed disruptions such as removal based on betweenness (Figure S1C,D), cascading (Figure S1E,F) and degree (Figure S1G,H; Table S4). The analysis of LCC size and APL before and after *Pseudomonas*'s removal provided insights into the network's resilience. In the OmMG network, LCC Size and APL values remained relatively unchanged, indicating stability (Figure S1I,J). However, in the OmSG network, differences in LCC size and APL values suggested that removing *Pseudomonas* could impact network stability (Figure S1K,L; Table S5).

The findings from the study underscore the nuanced but pivotal role of *Pseudomonas* in the Om microbiome, influencing both its structure and robustness.

3.2 | Impact of anti-microbiota vaccine on *O. moubata* fitness

To empirically test the hypothesis that targeting *Pseudomonas* could affect the fitness and microbiome of ticks feeding on rabbits, we conducted a vaccination experiment using *Pseudomonas*, a keystone species, and *Lactobacillus*, a non-keystone species (Figure 1). The rabbits' immune response to these vaccines was measured by checking the levels of IgG antibodies specific for each bacterium. From the fifteenth day after receiving the second dose of vaccine, the rabbits showed an increased antibody titres in both *Pseudomonas* and *Lactobacillus* of 1/6400 and 1/3200, respectively (Figure S2A,B), indicating successful vaccination. However, antibody levels were significantly higher only in the *Pseudomonas* group ($p < .05$) compared to the control group (Figure 3a). Cross-reactivity between the two groups was low in both cases, implying that there was no immune response against shared epitopes among the proteins of these bacteria (Figure 3a,b).

How the vaccinations affected ticks that fed on the vaccinated rabbits was evaluated. Notably, female ticks feeding on rabbits vaccinated with *Pseudomonas* showed a significant decrease in survival ($p < .01$), though this effect was not seen in male ticks or those feeding on *Lactobacillus*-vaccinated rabbits (Table 1). Furthermore, ticks feeding on rabbits vaccinated with *Lactobacillus* experienced reductions in both egg-laying and fertility rates, suggesting the vaccine influenced tick reproductive outcomes (Table 1). A slight decrease in the amount of blood ticks were able to ingest in both groups were observed, with the efficacy of the vaccines measured at 7.9% for *Pseudomonas* and 16.7% for *Lactobacillus* (Table 1).

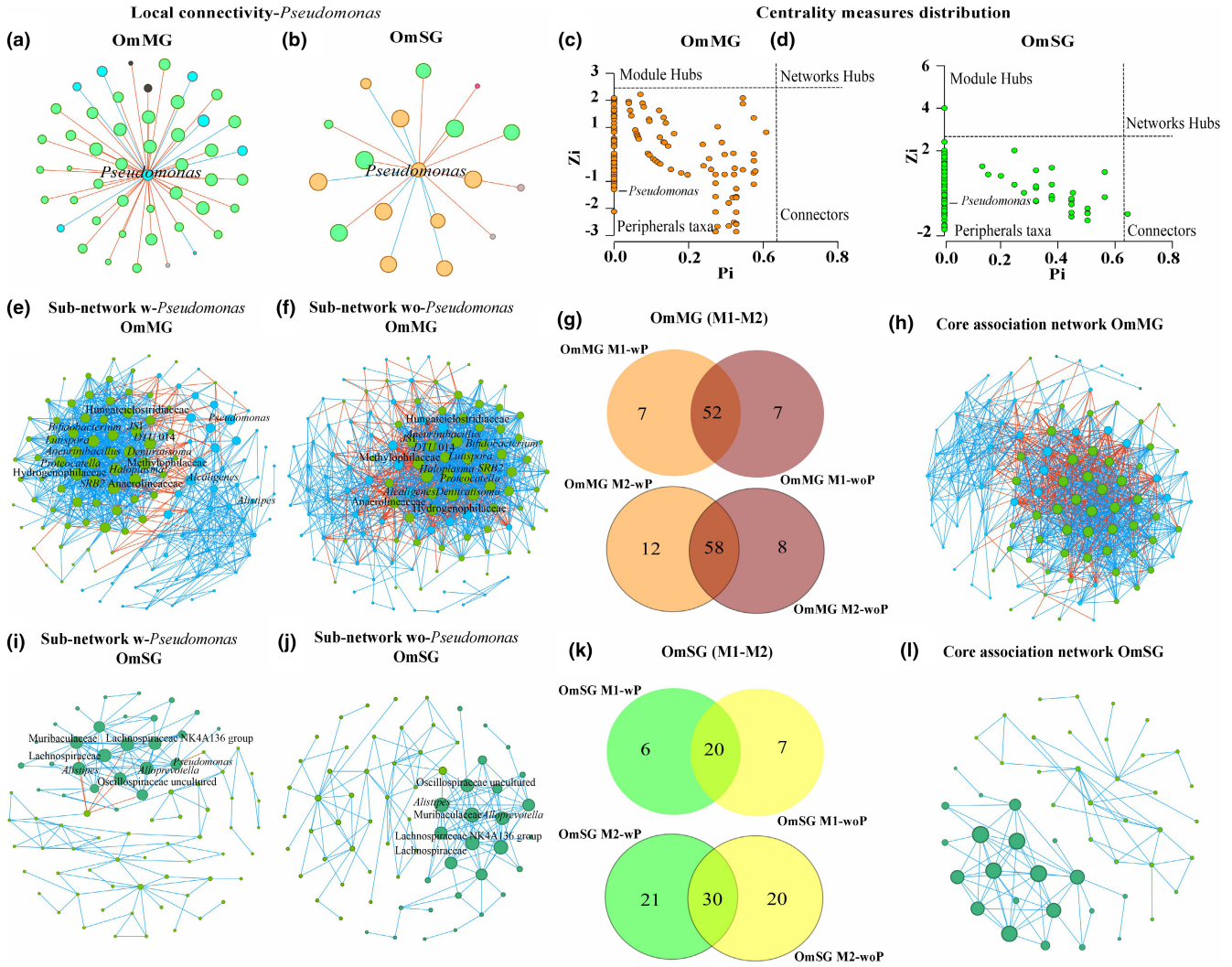

FIGURE 2 Assembly patterns of *Pseudomonas* in microbial communities of *O. moubata*. *Pseudomonas*'s local connectivity in: (a) OmMG and (b) OmSG. Within-module and among-module connectivities, Zi-Pi plot of the individual genera from four groups: (c) OmMG and (d) OmSG. Sub-networks of M1 and M2 in the presence and after *Pseudomonas*'s removal within *O. moubata* MG: (e) OmMG wP and (f) OmMG woP. (g) Venn diagram displaying the comparison of module composition in *O. moubata*-MG (M1-M2). (h) CAN for OmMG (wP-woP). Sub-networks of M1 and M2 in the presence and after *Pseudomonas*'s removal within *O. moubata*-SG: (i) OmSG wP and (j) OmSG woP. (k) Venn diagram displaying the comparison of module composition in *O. moubata*-SG (M1–M2). (l) CAN for OmSG (wP-woP). In the sub-networks the nodes represent bacterial taxa and the colours in the edges represent strong positive (blue) or negative (red) correlations (SparCC >0.75 or < −0.75).

3.3 | Impact of anti-microbiota vaccine on the diversity, composition and abundance of *O. moubata* microbiome

After vaccinating with *Pseudomonas* and *Lactobacillus*, the diversity, composition, and relative abundance of bacterial taxa in the OmMG using 16S rRNA gene profiling were examined. This analysis was done after identifying and removing DNA sequences deemed as contaminants (Table S6).

The findings revealed significant changes in the observed species richness (Figure 4a), Faith's phylogenetic diversity (Figure 4b), and evenness (Figure 4c). The results showed that all three-diversity metrics were significantly reduced in the OmMG-L group, indicating a less diverse bacterial community compared to both the OmMG-C and OmMG-P groups (Kruskal–Wallis, $p < .05$). This suggests that vaccination with *Lactobacillus* has a notable impact on reducing the variety and balance of bacterial species in the OmMG microbiome.

Analysis using the Bray–Curtis index highlighted significant differences in the bacterial community structure between the OmMG-C and OmMG-L groups (PERMANOVA, $p < .05$), as well as between the two vaccinated groups (PERMANOVA, $p < .01$), while no significant differences between the OmMG-C and OmMG-P groups (PERMANOVA, $p > .05$; Figure 4d,e). Pairwise comparisons of beta dispersion showed no significant variability between samples of the OmMG-P (ANOVA test, $p > .05$, Figure 4d) and OmMG-L

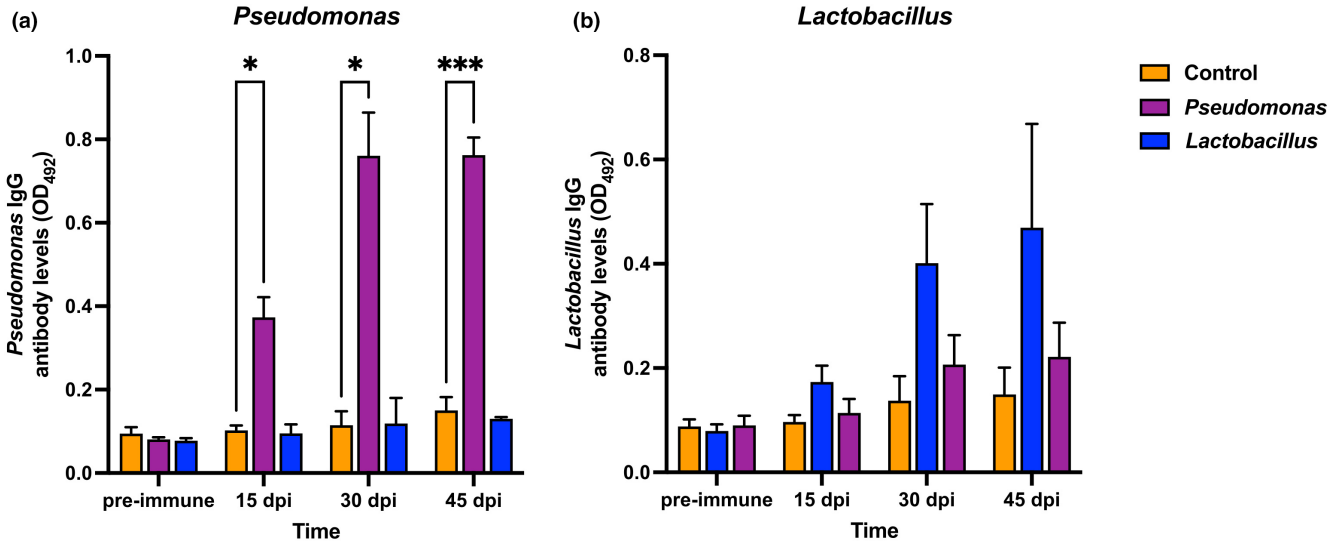

FIGURE 3 Antibody response in rabbits vaccinated with *Pseudomonas* or *Lactobacillus*. IgG antibody levels quantification against (a) *Pseudomonas* proteins and (b) *Lactobacillus* proteins. Values are the mean OD ± SD at 492 nm from each group. The comparative analysis of the results was performed using a two-way ANOVA, followed by the Bonferroni test for pairwise comparisons between control and immunized rabbits (*$p < .05$, ***$p < .001$). The sera were used at 1/100 dilution. Sera were taken before first antigen dose (pre-immune), 15 days post-inoculation immunization (dpi) with the first dose (15 dpi), 15 days after the second dose and before tick infestation (30 dpi), and 30 days after the second dose and 15 days after the tick challenge (45 dpi).

TABLE 1 Effect of the vaccination on *O. moubata* specimens fed on vaccinated rabbits with *Pseudomonas* and *Lactobacillus*.

Parameter	Developmental stage	Control	*Pseudomonas* (% change)	*Lactobacillus* (% change)
Ingested blood (mg)	Males	28.1 ± 3.1	27.0 ± 4.9 (3.9)	26.5 ± 0.7 (5.7)
	Females	225.0 ± 10.5	244.4 ± 16.6	209.8 ± 18.3 (6.8)
Survival (%)	Males	96.7 ± 3.3	100	100
	Females	100	93.3 ± 0.0 (6.7)**	100
Oviposition (number of eggs/female)	Females	274.6 ± 14.3	267.5 ± 13.6 (2.6)	226.6 ± 18.1 (17.5)**
Fertility (number of larvae/female)	Females	261.8 ± 11.1	258.5 ± 11.7 (1.3)	218.1 ± 16.1 (16.3)**
Efficacy (%)		–	7.9	16.7

Note: Bacteria were administered in Montanide ISA 71 VG. Results are shown as mean ± standard deviation for each rabbit group. Means were compared between ticks fed on vaccinated and control rabbits by one-way ANOVA followed by the Dunnett's *t*-test. In parentheses, % of reduction in the corresponding parameter respect to the control. Values $p < .05$ were considered significant (**$p < .01$).

(ANOVA test, $p > .05$, Figure 4e), with the control group. Jaccard clustering analysis showed two main clusters: one primarily composed of samples from OmMG-P group and another primarily from the OmMG-L group (Figure 4f).

The compositional analysis revealed a total of 152 bacterial taxa, with 44 (28.9%) shared across all samples (Figure 4g; Table S7). Notably, the OmMG-P group contained the largest number of unique bacterial taxa, followed by the control and OmMG-L groups, indicating that vaccination with *Pseudomonas* resulted in a more diverse bacterial population in the tick midgut (Figure 4g; Table S7).

Differential relative abundance analysis identified significant changes in four taxa (*Francisella*, *Methylobacterium-Methylorubrum*, *Phyllobacterium* and *Sphingobacterium*) across the three groups (Figure 4h; Table S8).

These findings indicate that vaccination with *Lactobacillus* had a more pronounced effect on the microbiome of the tick midgut compared to the control and *Pseudomonas* vaccination, affecting both the diversity and composition of bacterial taxa. The differences in the impact of vaccination with *Lactobacillus* and *Pseudomonas* suggest that the choice of vaccine can significantly influence the microbial community within the tick midgut.

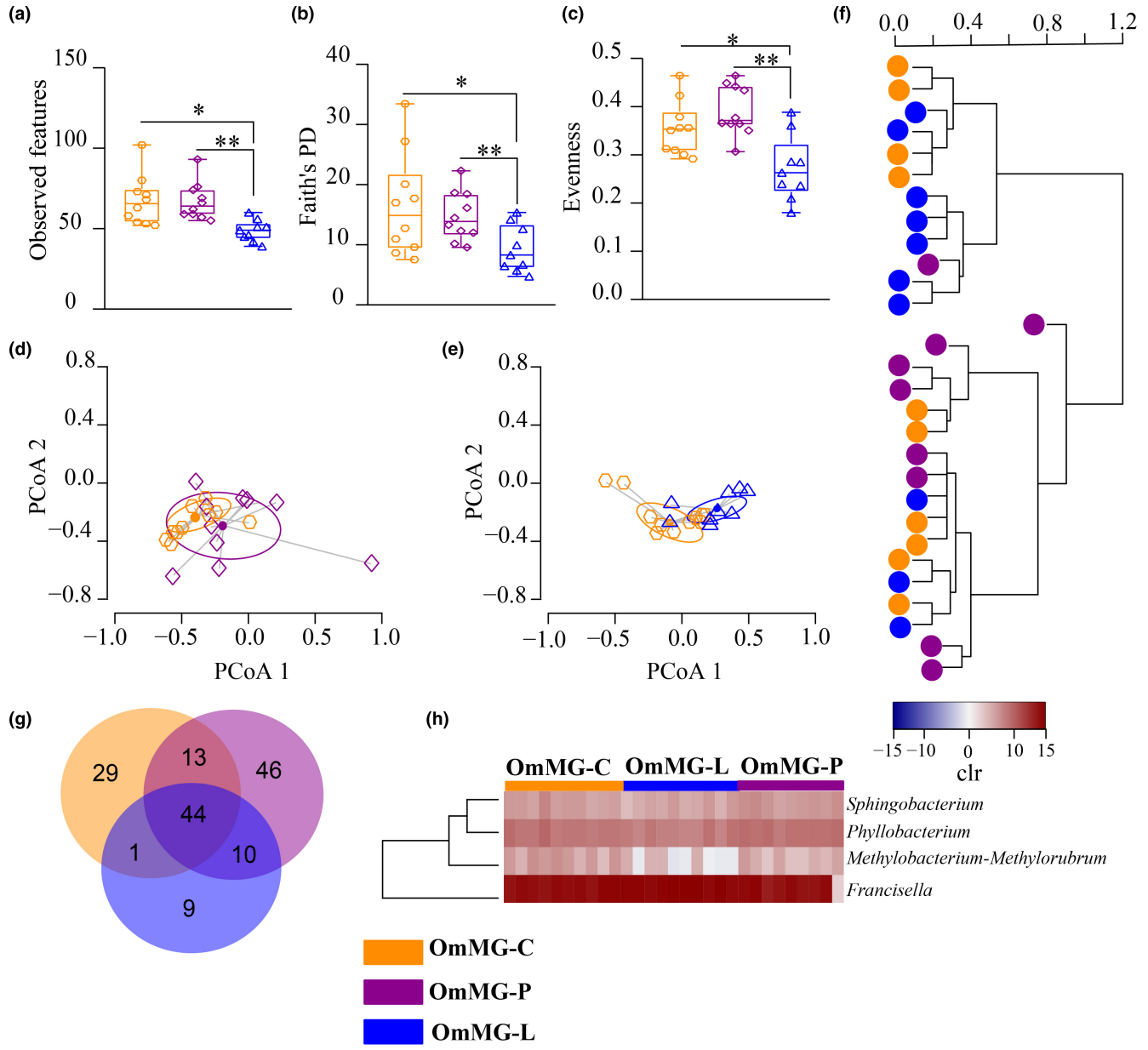

FIGURE 4 Impact of anti-microbiota vaccination on *O. moubata* microbiome diversity. Comparison of alpha diversity between OmMG-C, OmMG-P and OmMG-L group (Kruskal-Wallis test, significant differences for $p \leq .05$), (a) observed features, (b) Faith's phylogenetic diversity (PD), and (c) Pielou's evenness index. Comparison of beta—diversity with Bray Curtis dissimilarity index between: (d) OmMG-C and OmMG-P, (e) OmMG-C and OmMG-L group. Beta dispersion of three sets of samples (pairwise comparison). Small hexagons, rhombuses and triangles represent samples, and ellipses represent centroid position for each group. ANOVA test was performed and showed that beta dispersion of the three sets of samples (three conditions) is not significantly different (OmMG-C and OmMG-P, $p = .28$; OmMG-C and OmMG-L, $p = .68$). (f) Jaccard clusterization of OmMG-C, OmMG-P and OmMG-L samples. The samples are represented by circles and the groups by colours (legend). (g) Venn diagram displaying the comparison of taxa composition in OmMG-C, OmMG-P and OmMG-L groups. Common and unique taxa between the conditions are represented. (h) Comparison of relative abundance of bacterial communities between OmMG-C, OmMG-P and OmMG-L group. Colour represent the clr value (range from −15 to 15).

3.4 | Effect of anti-microbiota vaccine on the community assembly of the *O. moubata* microbiome

The study also explored if anti-microbiota vaccination also has an impact on the community assembly of the Om microbiome. To address this question, co-occurrence networks were built for each group, and compared using NetCoMi.

Upon visual inspection, the networks appeared similar across the groups (Figure 5a–c). However, the topological features showed differences between the networks (Table 2). Specifically, a reduction in the number of edges in OmMG-P and OmMG-L networks, compared to OmMG-C network. Additionally, the OmMG-P network not only had a greater number of taxa (nodes) but also exhibited a higher degree of connectivity among these nodes. Remarkably, the

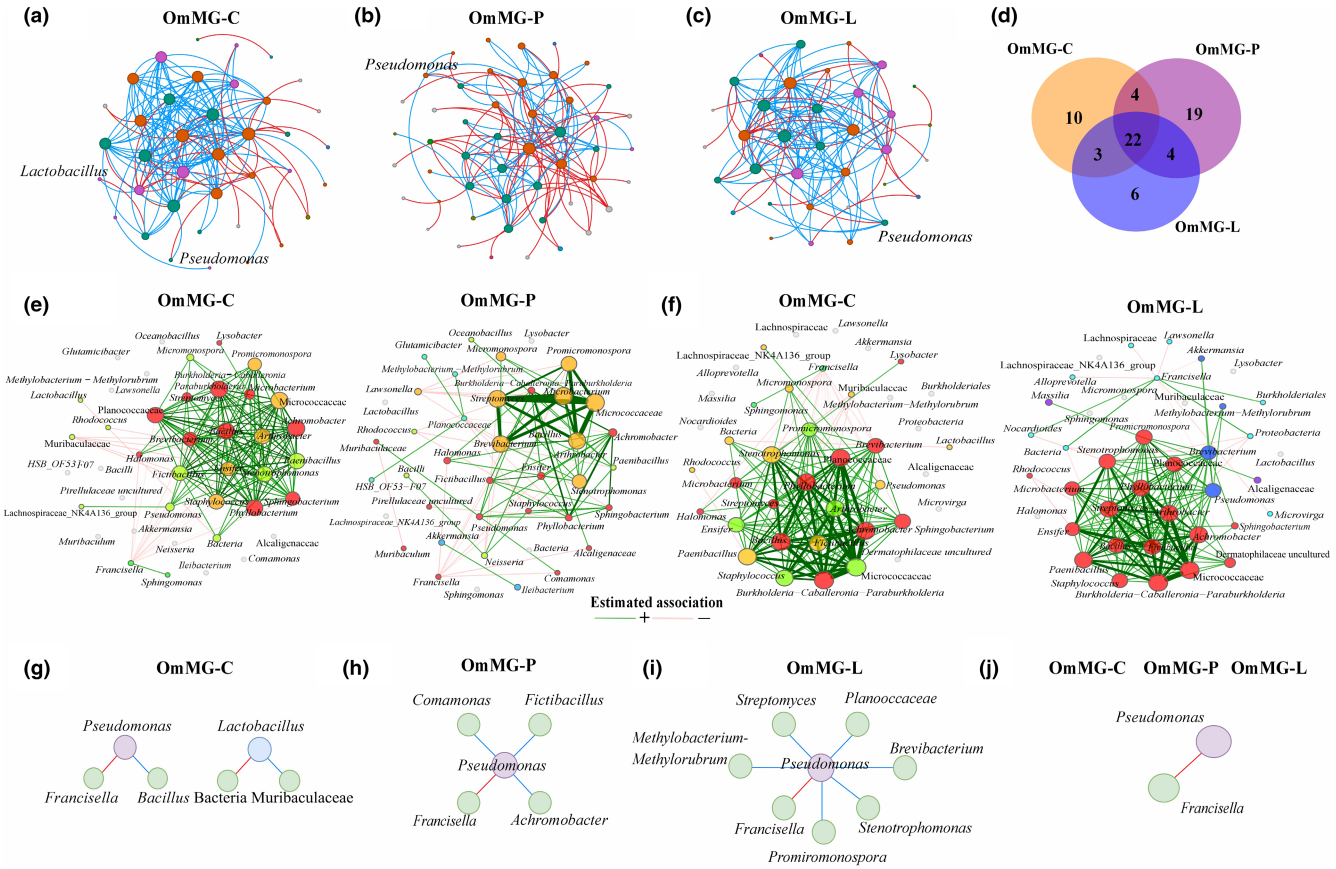

FIGURE 5 Impact of anti-microbiota vaccination on *O. moubata* community assembly. Co-occurrence networks of the (a) OmMG-C, (b) OmMG-P and (c) OmMG-L group. The positive and negative association are showed in blue and red, respectively. (d) Venn diagram represent the composition comparison of the vaccinated groups with the control group OmMG (C-P-L). Differential network comparison of vaccinated group to the OmMG-C group: (e) OmMG-C co-occurrence network and OmMG-P co-occurrence networks, (f) OmMG-C co-occurrence network and OmMG-L co-occurrence networks. The positive and negative association are showed in green and red, respectively. Directly connected nodes to *Pseudomonas* and *Lactobacillus* in: (g) OmMG-C, (h) OmMG-P and (i) OmMG-L group. (j) Common directly connected node to *Pseudomonas* in all three groups. The positive and negative association are shown in blue and red, respectively.

TABLE 2 Topological features for vaccinated (OmMG-P and OmMG-L) and OmMG-C networks.

Topological features	OmMG-C	OmMG-P	OmMG-L
Total nodes	87	112	64
Connected nodes	39	49	35
Edges	159	127	134
Positives	124 (78%)	65 (51.2%)	103 (76.9%)
Negatives	35 (22%)	62 (48.8%)	31 (23.1%)
Modularity	0.128	2.98	0.27
Network diameter	5	6	5
Average degree	8.15	5.18	7.66
Weighted degree	3.45	0.312	2.92
Clustering coefficient	0.73	0.62	0.64

modularity, a measure of the network's division into sub-networks, of the OmMG-P network was notably higher than the OmMG-C and OmMG-L networks. This suggests a more complex organization within the *Pseudomonas* group's microbiome. The OmMG-P network showed a higher number of unique nodes, compared to the others groups (Figure 5d; Table S9).

NetCoMi was used to compare the networks of vaccinated groups against a control (OmMG-C), focusing on *Pseudomonas* (OmMG-P; Figure 5e) and *Lactobacillus* (OmMG-L; Figure 5f). The analysis revealed that the network of the OmMG-P had fewer connections than OmMG-C, a difference also reflected in the network's topological characteristics (Table 2).

Networks were also compared in terms of the distribution of local centrality measures and clustering. The Jaccard index values of the comparisons OmMG-P versus OmMG-C, and OmMG-L versus OmMG-C were higher than expected by random, except for betweenness centrality in the OmMG-L versus OmMG-C comparison, which exhibited a random distribution (Table 3). The comparison of node clustering networks showed higher ARI values for OmMG-P compared to OmMG-C networks (ARI = 0.615), followed by OmMG-L/OmMG-C (ARI = 0.586), suggesting that the networks are more similar than expected by random. This implies that, although there are differences between the networks of vaccinated groups with the control group, there may be still shared

TABLE 3 Comparison of centrality measures between vaccinated (OmMG-P and OmMG-L) and OmMG-C groups.

	OmMG-P vs. OmMG-C			OmMG-L vs. OmMG-C		
Local centrality measures	**Jacc[a]**	***P*(≤Jacc)**	***P*(≥Jacc)**	**Jacc[a]**	***P*(≤Jacc)**	***P*(≥Jacc)**
Degree	0.561	0.999	0.002260**	0.525	0.996	0.009552**
Betweenness centrality	0.682	0.999	0.000879***	0.526	0.976	0.064766
Closeness centrality	0.561	0.999	0.002260**	0.525	0.996	0.009552**
Eigenvector centrality	0.561	0.999	0.002260**	0.525	0.996	0.009552**
Hub taxa	0.561	0.999	0.002260**	0.525	0.996	0.009552**

**$p < .01$, and ***$p < .001$.
[a]Jaccard index.

TABLE 4 Topological features for vaccinated (OmMG-P and OmMG-L) and OmMG-C sub-networks.

	Groups			
Topological features	**OmMG-C**		**OmMG-P**	**OmMG-L**
Node	*Pseudomonas*	*Lactobacillus*	*Pseudomonas*	*Pseudomonas*
Degree	2	2	5	7
Weighted degree	−0.056	−0.028	1.78	2.8
Closeness centrality	0.409	0.371	0.428	0.478
Betweenness centrality	0	0.125	115	13.74
Modularity class	5	2	3	0
Eigenvector centrality	0.09	0.079	0.252	0.36

patterns or relationships within the microbiome structure among these groups.

Co-occurrence sub-networks that highlight interactions specifically linked to *Pseudomonas* and *Lactobacillus* within each group was also analysed: OmMG-C (Figure 5g), OmMG-P (Figure 5h) and OmMG-L (Figure 5i). Interestingly, *Lactobacillus* was missing from its vaccination group (OmMG-L) as well as from the OmMG-P group, indicating that this taxon is particularly sensitive to the perturbation caused by anti-microbiota vaccines (Figure 5h,i). On the other hand, *Pseudomonas* showed a higher degree in the OmMG-P and OmMG-L groups compared to the OmMG-C (Figure 5g–i), with significantly higher betweenness and eigenvector centrality values (Table 4), indicating a pivotal role in the microbial network post-vaccination. The sub-networks were unique in their connections, with *Pseudomonas* uniquely positioned against *Francisella* across all networks (Figure 5j).

The results show a moderate but specific impact of each taxon on the assembly of the microbial community after vaccination. Changes in network configuration as a consequence of manipulating taxa suggest possible differences in the ability to resist external perturbations.

3.5 | Impact of anti-microbiota vaccine on network robustness

The robustness of networks from each group was analysed. When randomly removing nodes, all networks were equally impacted (Figure 6a; Table S10). However, the OmMG-L network showed the highest robustness against targeted removals based on betweenness (Figure 6b), cascading (Figure 6c) and degree (Figure 6d; Table S10). On the other hand, both the OmMG-C and OmMG-P networks experienced an 80% loss of connectivity after the removal of nearly 20% of their nodes, displaying a similar pattern of vulnerability (Figure 6b–d; Table S10).

To assess the impact of adding nodes, changes in the LCC size were measured (Figure 6e) and the APL (Figure 6f) within the networks (Table S11). The OmMG-P network proved to be more tolerant to nodes addition, as indicated by a larger LCC compared to OmMG-C and OmMG-L networks (Figure 6e; Table S11). Additionally, the APL remained consistent across all three networks following the addition of nodes (Figure 6f; Table S11), indicating a similar response to network expansion.

The robustness of the networks during the removal and not the addition of nodes suggests a stabilizing potential of *Lactobacillus* vaccination against the loss of bacterial taxa.

4 | DISCUSSION

This study introduces an innovative strategy using an anti-microbiota vaccine to target and modulate specific bacterial groups within the microbiome of soft ticks, leveraging host-generated antibodies. The ultimate aim of anti-microbiota vaccines is to alter vector physiology and their capacity to transmit pathogens (Maitre et al., 2022; Pavanelo et al., 2023; Wang et al., 2023; Wu-Chuang et al., 2022). Two bacterial targets were tested: *Pseudomonas*, the only common keystone bacterium previously identified in the MG and SG of the

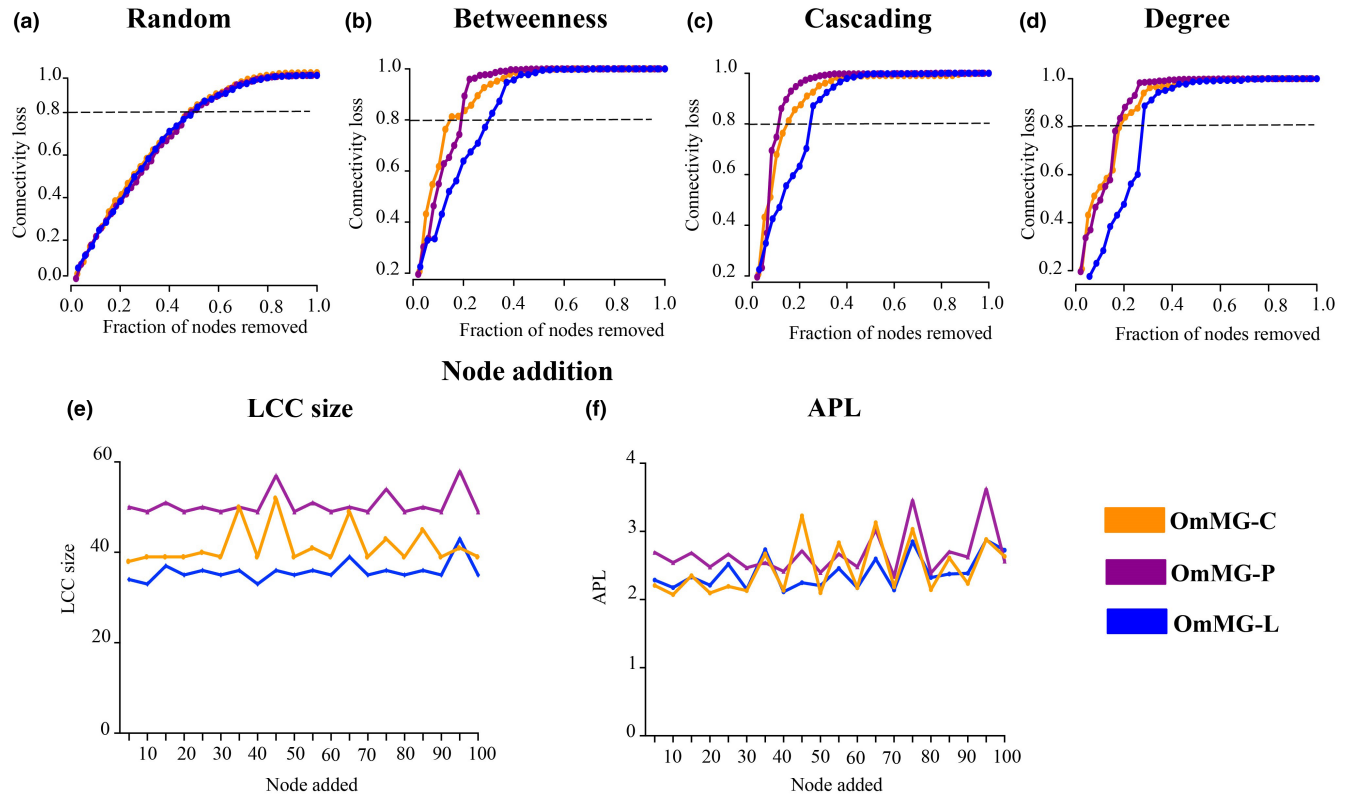

FIGURE 6 Impact of anti-microbiota vaccination on network robustness. Robustness test of the OmMG-C, OmMG-P and OmMG-L networks. Node removal directed attack based on (a) random, (b) betweenness, (c) cascading and (d) degree. Effect of node addition ($n = 100$) by measuring (e) LCC size and (f) APL.

tick species *O. moubata*, and *Lactobacillus*, an abundant but non-keystone bacterium in the same species, serving as a comparative control in the study.

The previous demonstration that the diversity, composition, abundance and assembly of microbial communities associated with *O. moubata* are tissue specific suggests different interaction patterns in OmMG and OmSG (Piloto-Sardiñas et al., 2023). Consequently, during the colonization process the taxa will not only have to face different physiological properties of each tissue but will also have to coexist with different microbial communities in terms of composition and interaction. In this context, the positioning of *Pseudomonas* as a common keystone taxon in both tissues (Piloto-Sardiñas et al., 2023) suggested an important role of the microorganism within the community since in theory the taxon faced different conditions and was still capable of carrying out an effective colonization process. The present findings revealed varied clustering patterns of *Pseudomonas* across different tissues, highlighting the bacterium's capacity to adjust its associations within microbial communities based on niche-specific conditions. This variability in clustering patterns may be influenced by the high microbial diversity found in Om, which is thought to be shaped by the anatomical and physiological variations in the midgut (Piloto-Sardiñas et al., 2023).

As a result of cooperative and co-exclusion interactions in ecological networks, microorganisms establish endogenous dynamics that can cause a damping effect against disturbances within ecosystems (Gonze et al., 2018; Konopka et al., 2015). The in silico analyses carried out revealed that *Pseudomonas* interacts extensively with diverse taxa, including keystone species, highlighting its significance in maintaining the microbial community structure. Microorganisms that form intricate ecological networks with the ability to shape entire communities are crucial (Mateos-Hernández et al., 2020). Despite being categorized as peripheral, *Pseudomonas* removal caused topological changes in sub-networks, demonstrating its nuanced yet influential role in the *O. moubata* microbiome, showcasing alterations in composition and connectivity patterns.

In both examined tissues, *Pseudomonas*, as keystone taxon, was observed to cluster with other keystone bacteria, some of which were present in lower numbers within the community. In any ecosystem, keystone species can exert a significant influence on their community, regardless of their numerical presence (Banerjee et al., 2018). However, identifying a bacterium as a key species does not necessarily confirm its impact on the microbial community (Banerjee et al., 2018). Therefore, the analysis of clustering and nesting patterns in complex ecological networks will allow predicting the effects of disturbances and the outcome of alterations such as consequence of the manipulation of taxa within the community (Deng et al., 2012; Xiao et al., 2017; Zhou et al., 2010).

These current findings align with previous research on the *O. moubata* microbiome (Piloto-Sardiñas et al., 2023), reinforcing the central role of *Pseudomonas* in tick microbial communities as a

promising target for interventions that influence the microbiome structure.

The influence of a keystone bacterium may become pivotal under specific conditions, which might differ from those under experimental investigation. This underscores the complexity of predicting and manipulating microbial community dynamics within ecological systems.

The empirical vaccination experiment targeting *Pseudomonas* and *Lactobacillus* in *O. moubata* revealed a successful immune response, indicated by increased IgG antibody levels. *Pseudomonas* vaccination elicited significantly higher antibody titres, emphasizing its robustness. Female ticks feeding on *Pseudomonas*-vaccinated rabbits exhibited increased mortality, while *Lactobacillus* vaccination affected tick reproductive outcomes, with reduced egg-laying and fertility rates. Recent studies indicate that manipulating keystone taxa within *I. ricinus* can alter the fitness of hard ticks (Mateos-Hernández et al., 2020). Our results suggest that, although moderate, selective manipulation of *Pseudomonas* and *Lactobacillus* has a direct influence on tick physiology or indirectly through interactions with other taxa.

The distinct gender-specific and reproductive impacts highlight the potential of microbiota-driven vaccines in tick population control. The observed variations in blood-feeding efficacy, along with differential vaccine efficacy (7.9% for *Pseudomonas* and 16.7% for *Lactobacillus*), emphasize the importance of specific microbial targets in vaccine development. These differential responses underscore the importance of understanding the microbiome dynamics within the tick host and the potential for precision in developing effective tick control strategies. Also, the vaccination experiment demonstrated the efficacy of microbiota-driven vaccines in influencing tick fitness and reproductive capabilities.

Despite being considered a keystone taxon, experimental manipulation of the OmMG microbiome with *Pseudomonas* did not result in significant changes in microbial diversity and community configuration compared to the control group. Conversely, immunization with *Lactobacillus* led to a reduction in microbial diversity compared to the control groups. These findings differ from experimental analyses conducted in *I. ricinus*, where immunization with a keystone taxon resulted in a more pronounced decrease in microbial diversity and alterations in community assembly compared to the effects of a non-keystone taxon (Mateos-Hernández et al., 2021). The perturbation of the OmMG microbiome through vaccination with *Pseudomonas* did not induce substantial changes in the diversity, composition and assembly of the microbial community. *Pseudomonas* species have a versatile metabolism, diverse capacity for enzyme production and rapid growth in sustainable carbon sources, making them resistant to extreme environments and external perturbations (Wang et al., 2020). These traits of the bacterial genus may clarify why *Pseudomonas* occupies a unique position, underscoring its pivotal role.

The considerable decrease in microbial diversity caused by vaccination with *Lactobacillus* and the absence in its own group and the *Pseudomonas* group indicated a specific response to vaccination with the taxon. The implication of these findings suggests that anti-microbiota vaccination induces specific alterations in microbial community dynamics within the tick midgut. Understanding the structure of microbial communities after vaccination is crucial for optimizing strategies to control tick populations and reduce the risk of tick-borne diseases.

Due to community assembly, biodiversity, heterogeneity, functional diversity and microbial interactions within ecosystems, microbial communities demonstrate resilience against fluctuating environmental conditions (Lee et al., 2023; Stenuit & Agathos, 2015). The evaluation of microbial network robustness post-anti-microbiota vaccination in *O. moubata* midgut (OmMG) revealed distinct patterns. The varied responses in robustness and tolerance to node removal or addition indicate that the selection of a vaccine affects the structural adaptability of the microbial network in the tick midgut. Interestingly, during node removal, the OmMG-L network was more robust than OmMG-P and OmMG-C networks. In ecosystems, there is a strong correlation between species diversity, microbial interactions and resistance to external disturbances. Therefore, theoretically, higher biodiversity would increase the community stability (Ratzke et al., 2020). On the contrary, our findings revealed that despite the loss of microbial diversity, the resilience of the OmMG-L network against targeted removals increased, suggesting a potential stabilizing effect of *Lactobacillus* vaccination. One potential explanation is that if the remaining members are capable of sustaining the ecosystem function previously carried out by the displaced taxa, the stability of the community may remain unaffected. Conversely, the robustness of the OmMG-P network to node addition may imply a more adaptable and resilient microbial community following *Pseudomonas* vaccination. This provides valuable insights for optimizing interventions aimed at manipulating tick microbial communities.

The synergy between in silico analyses and empirical vaccination experiments enhances the validity of the study's outcomes. The study has elucidated the intricate dynamics of the Om microbiome, emphasizing the pivotal role of *Pseudomonas*, a keystone taxon in tick midgut, in shaping microbial networks. Vaccination against the microbiota, specifically targeting *Pseudomonas*, demonstrates potential in controlling tick fitness, impacting microbiome structure and changing community assembly. The intricate interactions within the tick microbiome emphasize the necessity of a holistic approach in developing effective strategies for tick-borne disease control.

Thus, the findings reported herein support the development of targeted microbiota-driven vaccines as effective strategies for controlling tick-borne diseases.

AUTHOR CONTRIBUTIONS

A.C.C., R.P.-S. and A.O. conceived the idea and designed experiments. A.L.C.-A., L.M.-H. and A.O. conducted the experiments. A.C.C., R.P.-S. and A.O. supervised the work. A.C.C. and R.P.-S. provided resources. A.L.C.-A., E.P.S., A.M., L.M.-H., J.M., A.W.-C., L.A.D., R.P.-S., A.O. and A.C.-C. analysed and/or interpreted the results. L.M.-H. performed formal analysis. E.P.S. visualized the results. D.O. provided software. A.L.C.-A., E.P.S. and A.C.C. drafted the first version of the manuscript. A.L.C.-A., E.P.S., A.M., L.M.-H., J.M., A.W.-C., L.A.D., D.O., T.B., A.O., R.P.-S. and A.C.-C. reviewed, edited and approved the manuscript.

ACKNOWLEDGEMENTS

UMR BIPAR is supported by the French Government's Investissement d'Avenir program, Laboratoire d'Excellence 'Integrative Biology of Emerging Infectious Diseases' (grant no. ANR-10-LABX-62-IBEID). The tasks performed by researchers at IRNASA was supported by the Spanish Ministry of Science, Innovation and Universities, the State Research Agency (AEI), the European Regional Development Fund (ERDF) (grant PID2022-136644OB-I00), and Spanish National Research Council (CSIC) (grant 22AEP1). In addition, ALC-A was supported by project 'CLU-2019-05-IRNASA/CSIC Unit of Excellence', granted by the Junta de Castilla y León and co-financed by the European Union (ERDF). AW-C is supported by Programa Nacional de Becas de Postgrado en el Exterior 'Don Carlos Antonio López' (grant no. 205/2018). Apolline Maitre is supported by the 'Collectivité de Corse', grant: 'Formations superieures' (SGCE—RAPPORT No 0300). AI technologies were used to improve spelling, grammar and general editing of the text. AI technologies were not used to produce scientific insights, or drawing scientific conclusions.

CONFLICT OF INTEREST STATEMENT

The authors declare no competing interests.

DATA AVAILABILITY STATEMENT

The datasets used and generated and analysed during the current study are available on the SRA repository (Bioproject No. PRJNA931807, PRJNA1035006).

ETHICS STATEMENT

Tick feeding procedures and the experiments involving rabbits received approval from the Ethical and Animal Welfare Committee of the Institute of Natural Resources and Agrobiology (IRNASA) and the Ethical Committee of the Spanish National Research Council (CSIC, Spain), under Permit Number 742/2017, and were conducted in compliance with the applicable EU legislation (Directive 2010/63/EU).

BENEFIT–SHARING STATEMENT

All collaborators are included as co-authors. The research addresses a priority concern, in this case novel vaccines for the control of ticks and tick-borne diseases. More broadly, our group is committed to international scientific partnerships, as well as institutional capacity building.

ORCID

Dasiel Obregón https://orcid.org/0000-0002-5786-1114
Alejandro Cabezas-Cruz https://orcid.org/0000-0002-8660-730X

REFERENCES

Acedo-Felix, E., & Gaspar Perez-Martınez, G. (2003). Significant differences between *Lactobacillus casei* subsp. casei ATCC 393T and a commonly used plasmid-cured derivative revealed by a polyphasic study. *International Journal of Systematic and Evolutionary Microbiology*, *53*, 67–75.

Aželytė, J., Wu-Chuang, A., Žiegytė, R., Platonova, E., Mateos-Hernandez, L., Maye, J., Obregon, D., Palinauskas, V., & Cabezas-Cruz, A. (2022). Anti-microbiota vaccine reduces avian malaria infection within mosquito vectors. *Frontiers in Immunology*, *13*, 841835.

Banerjee, S., Schlaeppi, K., & van der Heijden, M. G. (2018). Keystone taxa as drivers of microbiome structure and functioning. *Nature Reviews Microbiology*, *16*(9), 567–576.

Bastian, M., Heymann, S., & Jacomy, M. (2009). Gephi: An open source software for exploring and manipulating networks. *Proceedings of the International AAAI Conference on Web and Social Media*, *3*(1), 361–362. https://doi.org/10.1609/icwsm.v3i1.13937

Bolyen, E., Rideout, J. R., Dillon, M. R., Bokulich, N. A., Abnet, C. C., Al-Ghalith, G. A., Alexander, H., Alm, E. J., Arumugam, M., Asnicar, F., Bai, Y., Bisanz, J. E., Bittinger, K., Brejnrod, A., Brislawn, C. J., Brown, C. T., Callahan, B. J., Caraballo-Rodríguez, A. M., Chase, J., … Caporaso, J. G. (2019). Reproducible, interactive, scalable and extensible microbiome data science using QIIME 2. *Nature Biotechnology*, *37*(8), 852–857.

Bray, J. R., & Curtis, J. T. (1957). An ordination of the upland forest communities of southern Wisconsin. *Ecological Monographs*, *27*(4), 326–349.

Callahan, B. J., McMurdie, P. J., Rosen, M. J., Han, A. W., Johnson, A. J. A., & Holmes, S. P. (2016). DADA2: High-resolution sample inference from Illumina amplicon data. *Nature Methods*, *13*(7), 581–583.

Cao, X., Zhao, D., Xu, H., Huang, R., Zeng, J., & Yu, Z. (2018). Heterogeneity of interactions of microbial communities in regions of Taihu Lake with different nutrient loadings: A network analysis. *Scientific Reports*, *8*(1), 8890.

Carnero-Morán, Á., Oleaga, A., Cano-Argüelles, A. L., & Pérez-Sánchez, R. (2023). Function-guided selection of salivary antigens from *Ornithodoros erraticus* argasid ticks and assessment of their protective efficacy in rabbits. *Ticks and Tick-borne Diseases*, *14*(6), 102218.

Cutler, S. J., Abdissa, A., & Trape, J. F. (2009). New concepts for the old challenge of African relapsing fever borreliosis. *Clinical Microbiology and Infection*, *15*(5), 400–406.

Davis, N. M., Proctor, D. M., Holmes, S. P., Relman, D. A., & Callahan, B. J. (2018). Simple statistical identification and removal of contaminant sequences in marker-gene and metagenomics data. *Microbiome*, *6*, 1–14.

Deng, Y., Jiang, Y. H., Yang, Y., He, Z., Luo, F., & Zhou, J. (2012). Molecular ecological network analyses. *BMC Bioinformatics*, *13*, 1–20.

DeSantis, T. Z., Hugenholtz, P., Larsen, N., Rojas, M., Brodie, E. L., Keller, K., Huber, T., Dalevi, D., Hu, P., & Andersen, G. L. (2006). Greengenes, a chimera-checked 16S rRNA gene database and workbench compatible with ARB. *Applied and Environmental Microbiology*, *72*(7), 5069–5072.

Diaz-Martin, V., Manzano-Román, R., Obolo-Mvoulouga, P., Oleaga, A., & Pérez-Sánchez, R. (2015). Development of vaccines against Ornithodoros soft ticks: An update. *Ticks and Tick-borne Diseases*, *6*(3), 211–220.

Faith, D. P. (1992). Conservation evaluation and phylogenetic diversity. *Biological Conservation*, *61*, 1–10.

Fernandes, A. D., Macklaim, J. M., Linn, T. G., Reid, G., & Gloor, G. B. (2013). ANOVA-like differential expression (ALDEx) analysis for mixed population RNA-seq. *PLoS One*, *8*(7), e67019.

Freitas, S., Yang, D., Kumar, S., Tong, H., & Chau, D. H. (2021). Evaluating graph vulnerability and robustness using tiger. In *Proceedings of the 30th ACM International Conference on Information & Knowledge Management (CIKM '21)* (pp. 4495–4503). Association for Computing Machinery. https://doi.org/10.1145/3459637.3482002

Friedman, J., & Alm, E. J. (2012). Inferring correlation networks from genomic survey data. *PLoS Computational Biology*, *8*(9), e1002687. https://doi.org/10.1371/JOURNAL.PCBI.1002687

García-Varas, S., Manzano-Román, R., Fernández-Soto, P., Encinas-Grandes, A., Oleaga, A., & Pérez-Sánchez, R. (2010). Purification and characterisation of a P-selectin-binding molecule from the salivary glands of *Ornithodoros moubata* that induces protective anti-tick immune responses in pigs. *International Journal for Parasitology*, *40*(3), 313–326.

Gonze, D., Coyte, K. Z., Lahti, L., & Faust, K. (2018). Microbial communities as dynamical systems. *Current Opinion in Microbiology*, *44*, 41–49.

Guimerà, R., & Nunes Amaral, L. A. (2005). Functional cartography of complex metabolic networks. *Nature*, *433*(7028), 895–900.

Guo, B., Zhang, L., Sun, H., Gao, M., Yu, N., Zhang, Q., Mou, A., & Liu, Y. (2022). Microbial co-occurrence network topological properties link with reactor parameters and reveal importance of low-abundance genera. *npj Biofilms and Microbiomes*, *8*(1), 3.

Katoh, K., & Standley, D. M. (2013). MAFFT multiple sequence alignment software version 7: Improvements in performance and usability. *Molecular Biology and Evolution*, *30*(4), 772–780. https://doi.org/10.1093/MOLBEV/MST010

Konopka, A., Lindemann, S., & Fredrickson, J. (2015). Dynamics in microbial communities: Unraveling mechanisms to identify principles. *The ISME Journal*, *9*(7), 1488–1495.

Lee, K. K., Park, Y., & Kuehn, S. (2023). Robustness of microbiome function. *Current Opinion in Systems Biology*, *36*, 100479. https://doi.org/10.1016/j.coisb.2023.100479

Lhomme, S. (2015). *NetSwan: Network strengths and weaknesses analysis. R Package Version 0.1*.

Maitre, A., Wu-Chuang, A., Aželytė, J., Palinauskas, V., Mateos-Hernández, L., Obregon, D., Hodžić, A., Valiente Moro, C., Estrada-Peña, A., Paoli, J. C., Falchi, A., & Cabezas-Cruz, A. (2022). Vector microbiota manipulation by host antibodies: The forgotten strategy to develop transmission-blocking vaccines. *Parasites & Vectors*, *15*(1), 1–12.

Maitre, A., Wu-Chuang, A., Mateos-Hernández, L., Piloto-Sardiñas, E., Foucault-Simonin, A., Cicculli, V., Moutailler, S., Paoli, J. C., Falchi, A., Obregón, D., & Cabezas-Cruz, A. (2023). Rickettsial pathogens drive microbiota assembly in *Hyalomma marginatum* and Rhipicephalus bursa ticks. *Molecular Ecology*, *32*(16), 4660–4676.

Mateos-Hernández, L., Obregón, D., Maye, J., Borneres, J., Versille, N., de La Fuente, J., Estrada-Peña, A., Hodžić, A., Šimo, L., & Cabezas-Cruz, A. (2020). Anti-tick microbiota vaccine impacts *Ixodes ricinus* performance during feeding. *Vaccine*, *8*(4), 702.

Mateos-Hernández, L., Obregon, D., Wu-Chuang, A., Maye, J., Bornères, J., Versillé, N., de la Fuente, J., Díaz-Sánchez, S., Bermúdez-Humarán, L. G., Torres-Maravilla, E., Estrada-Peña, A., Hodžić, A., Šimo, L., & Cabezas-Cruz, A. (2021). Anti-microbiota vaccines modulate the tick microbiome in a taxon-specific manner. *Frontiers in Immunology*, *12*, 704621.

Oksanen, J., Simpson, G. L., Blanchet, G., Kindt, R., Legendre, P., Minchin, P. R., O'Hara, R. B., Solymos, P., Stevens, H. M. H., Szöcs, E., Wagner, H. H., Barbour, M., Bedward, M., Bolker, B., Borcard, D., Carvalho, G., Chirico, M., De Cáceres, M., Durand, S., … Weedom, J. (2021). Vegan: Community ecology package. R package version 2.6-0.

Pavanelo, D., Piloto-Sardiñas, E., Maitre, A., Abuin-Denis, L., Kopáček, P., Cabezas-Cruz, A., & Fogaça, A. (2023). Arthropod microbiota: Shaping pathogen establishment and enabling control. *Frontiers in Arachnid Science*, *2*, 1297733.

Peschel, S., Müller, C. L., Von Mutius, E., Boulesteix, A. L., & Depner, M. (2021). NetCoMi: Network construction and comparison for microbiome data in R. *Briefings in Bioinformatics*, *22*(4), bbaa290.

Pielou, E. C. (1966). The measurement of diversity in different types of biological collections. *Journal of Theoretical Biology*, *13*, 131–144.

Piloto-Sardiñas, E., Cano-Argüelles, A. L., Maitre, A., Wu-Chuang, A., Mateos-Hernández, L., Corduneanu, A., Obregón, D., Oleaga, A., Pérez-Sánchez, R., & Cabezas-Cruz, A. (2023). Comparison of salivary gland and midgut microbiome in the soft ticks *Ornithodoros erraticus* and *Ornithodoros moubata*. *Frontiers in Microbiology*, *14*, 1173609.

Price, M. N., Dehal, P. S., & Arkin, A. P. (2010). FastTree 2–approximately maximum-likelihood trees for large alignments. *PLoS One*, *5*(3), e9490.

Qi, Y., Zhang, J., André, M. R., & Qin, T. (2024). New insights in the microbe-vector interaction. *Frontiers in Microbiology*, *15*, 1364989.

Quast, C., Pruesse, E., Yilmaz, P., Gerken, J., Schweer, T., Yarza, P., Peplies, J., & Glöckner, F. O. (2012). The SILVA ribosomal RNA gene database project: Improved data processing and web-based tools. *Nucleic Acids Research*, *41*(D1), D590–D596.

R Core Team. (2023). *R: A language and environment for statistical computing*. R Foundation for Statistical Computing. https://www.R-project.org/

Ratzke, C., Barrere, J., & Gore, J. (2020). Strength of species interactions determines biodiversity and stability in microbial communities. *Nature Ecology & Evolution*, *4*(3), 376–383.

Röttjers, L., Vandeputte, D., Raes, J., & Faust, K. (2021). Null-model-based network comparison reveals core associations. *ISME Communications*, *1*(1), 36.

RStudio Team. (2020). *RStudio: Integrated development environment for R*. RStudio, PBC. http://www.rstudio.org/

Stenuit, B., & Agathos, S. N. (2015). Deciphering microbial community robustness through synthetic ecology and molecular systems synecology. *Current Opinion in Biotechnology*, *33*, 305–317.

Wang, J., Gao, L., & Aksoy, S. (2023). Microbiota in disease-transmitting vectors. *Nature Reviews Microbiology*, *21*, 1–15.

Wang, S., Cui, J., Bilal, M., Hu, H., Wang, W., & Zhang, X. (2020). *Pseudomonas* spp. as cell factories (MCFs) for value-added products: From rational design to industrial applications. *Critical Reviews in Biotechnology*, *40*(8), 1232–1249.

Wu-Chuang, A., Hodžić, A., Mateos-Hernández, L., Estrada-Peña, A., Obregon, D., & Cabezas-Cruz, A. (2021). Current debates and advances in tick microbiome research. *Current Research in Parasitology & Vector-Borne Diseases*, *1*, 100036.

Wu-Chuang, A., Mateos-Hernandez, L., Maitre, A., Rego, R. O., Šíma, R., Porcelli, S., … Cabezas-Cruz, A. (2023). Microbiota perturbation by anti-microbiota vaccine reduces the colonization of *Borrelia afzelii* in *Ixodes ricinus*. *Microbiome*, *11*(1), 151.

Wu-Chuang, A., Obregon, D., Mateos-Hernández, L., & Cabezas-Cruz, A. (2022). Anti-tick microbiota vaccines: How can this actually work? *Biologia*, *77*(6), 1555–1562.

Xiao, Y., Angulo, M. T., Friedman, J., Waldor, M. K., Weiss, S. T., & Liu, Y. Y. (2017). Mapping the ecological networks of microbial communities. *Nature Communications*, *8*(1), 2042.

Zheng, D., Liwinski, T., & Elinav, E. (2020). Interaction between microbiota and immunity in health and disease. *Cell Research*, *30*(6), 492–506.

Zhou, J., Deng, Y., Luo, F., He, Z., Tu, Q., & Zhi, X. (2010). Functional molecular ecological networks. *MBio*, *1*(4), 10–1128.

SUPPORTING INFORMATION

Additional supporting information can be found online in the Supporting Information section at the end of this article.

How to cite this article: Cano-Argüelles, A. L., Piloto-Sardiñas, E., Maitre, A., Mateos-Hernández, L., Maye, J., Wu-Chuang, A., Abuin-Denis, L., Obregón, D., Bamgbose, T., Oleaga, A., Cabezas-Cruz, A., & Pérez-Sánchez, R. (2024). Microbiota-driven vaccination in soft ticks: Implications for survival, fitness and reproductive capabilities in *Ornithodoros moubata*. *Molecular Ecology*, *00*, e17506. https://doi.org/10.1111/mec.17506